

Supporting Information

Classification of crystal structures of extended aromatic hydrocarbons and the systematic relations

Takehiko Mori

Department of Materials Science and Engineering, Tokyo Institute of Technology, Ookayama 2-12-1, Meguro-ku, Tokyo 152-8552, Japan. E-mail: mori.t@mac.titech.ac.jp

Parameters of intermolecular interaction

To define the molecular coordinates (X, Y, Z) (Fig. 1(g)), the molecular center (x_0, y_0, z_0) was estimated from the rectangular coordinates (x, y, z) of a molecule obtained from the reported crystal data. Then, six elements of the moment,

$$\langle xx \rangle = \sum (x - x_0)^2, \langle xy \rangle = \sum (x - x_0)(y - y_0), \text{ etc.} \quad (\text{S1})$$

were calculated. After the diagonalization of the 3×3 matrix, (X, Y, Z) were obtained by multiplying the eigenvectors to $(x - x_0, y - y_0, z - z_0)$. The resulting molecular coordinates, (X, Y, Z), were oriented along the molecular long, short, and vertical axes, respectively (Fig. 1(g)). The moments were calculated from all non-hydrogen atoms, but the alkyl groups and the substituents were not included. For the SHB molecules in Table 1, the X axis was defined so as to coincide with the vertical direction of Fig. 3.

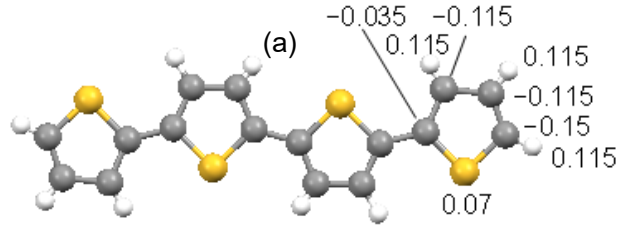
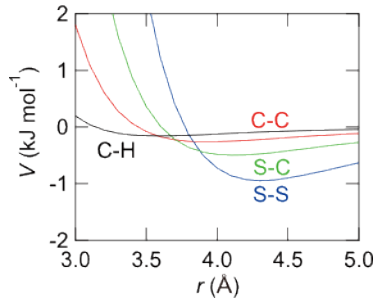
The intermolecular energy was estimated according to the standard 6-exp potential,^{S1-S8}

$$V = \varepsilon \left[A \exp \left(-B \frac{r}{r_0} \right) - C \left(\frac{r_0}{r} \right)^6 \right] + D \rho_i \rho_j / r \quad (\text{S2})$$

where $A = 184000$, $B = 12$, $C = 2.25$, and $D = 1380 \text{ kJ } \text{\AA} \text{ mol}^{-1}$.^{S9} The parameters were taken from the MM3 force field (Table S1).^{12,23,S10} The dispersion represented by this equation has a minimum of 1.12ε at r_0 (Fig. S1(a)). For interaction between different atoms, the geometrical average was used for ε , while the arithmetic average was used for r_0 . There were no reliable parameters for Se, but the values that gave slightly larger potentials than S were used. To this dispersion energy, electrostatic energy coming from the last term was added.^{S3-S5,S8} Charges ρ_i calculated from the molecular orbitals scattered largely,¹² and significantly depended on the estimation methods, hence the same charge was allotted to the same kind of atoms (Table S1). The opposite charge was allotted to the connecting carbon atoms so as to maintain the charge neutrality (Fig. S1(b)). Charges on N and S were either positive or negative depending on the environments, so the average values were adopted. The results reproduced the reported charges well.¹² Usually, electrostatic energy between various atoms canceled each other, and the total electrostatic contribution was less than 10% of the total intermolecular energy (Fig. 2(a)).

Table S1 Force-field parameters^{S10}

Atom	ϵ (kJ mol ⁻¹)	r_0 (Å)	Charge ρ_i
C	0.2343	3.92	–
H	0.0837	3.24	0.115
O	0.2466	3.64	–0.30
S	0.8452	4.30	0.07
N	0.1797	3.86	0.00

Fig. S1 (a) Potential curves based on eq (5) and Table S1. (b) Charges on 4T.

Criterion (b)
between the HB and

stacking structures

The criterion (dashed line in Fig. 2(f)) is represented as

$$\frac{V_{g\text{ stat}}(60) - V_{s\text{ stat}}(180)}{2V_{g\text{ vdW}}(60) - V_{s\text{ vdW}}(180)} = 0.25 \quad (\text{S3})$$

In general, the total energies at 60° and 180° are

$$V_t(60) = 2V_g(60) + V_s(60) \quad (\text{S4})$$

$$V_t(180) = 2V_g(180) + V_s(180) \quad (\text{S5})$$

When eqn (S5) is subtracted from eqn (S4),

$$V_t(60) - V_t(180) = [2V_g(60) - V_s(180)] + [V_s(60) - 2V_g(180)] \quad (\text{S6})$$

If the second term is neglected, and $V_t = V_{\text{vdW}} + V_{\text{stat}}$ is used,

$$V_t(60) - V_t(180) = 2V_{g\text{ vdW}}(60) \left(1 + \frac{V_{g\text{ stat}}(60)}{V_{g\text{ vdW}}(60)} \right) - V_{s\text{ vdW}}(180) \left(1 + \frac{V_{s\text{ stat}}(180)}{V_{s\text{ vdW}}(180)} \right) \quad (\text{S7})$$

If $2V_{g\text{ vdW}}(60) = V_{s\text{ vdW}}(180)$, this equation leads to the left-hand side of eqn (S3). The actual values (divided by N_{core}) are $V_s(60) - 2V_g(180) = 0.21$ kJ mol⁻¹, $2V_{g\text{ vdW}}(60) - V_{s\text{ vdW}}(180) = 0.05$ kJ mol⁻¹, and $V_{g\text{ vdW}}(60) = -1.6$ kJ mol⁻¹ for pentacene (Fig. 2(a)). Then, eqn (S3) is a reasonable relation.

Table S2 Supplementary structure parameters of the third interactions

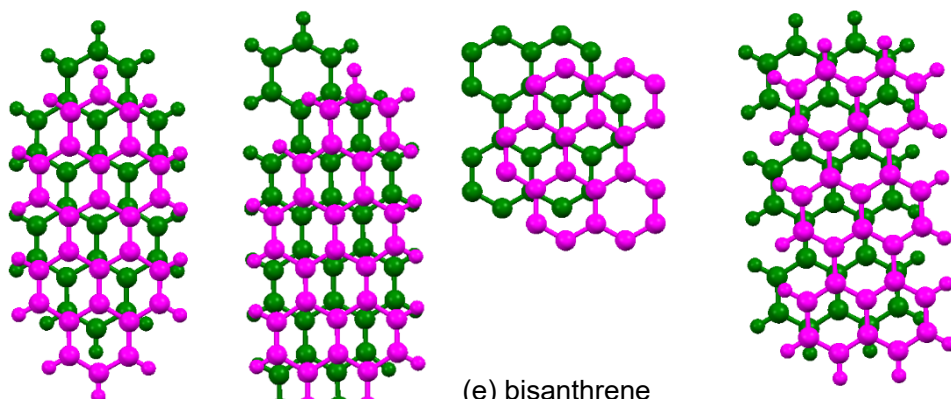
Compound	μ_{\max}^a ($\text{cm}^2\text{V}^{-1}\text{s}^{-1}$)	b (Å)	θ (°)	X_p (Å)	Y_p (Å)	Z_p (Å)	V_p (kJ mol ⁻¹)
θ							
θ -bisanthrene		4.1842	30.2	5.29	9.57	0.57	-10.40
tetracenotetracene		3.8311	128.7	6.57	6.52	2.33	-23.89
flavanthrene		3.7996	132.0	13.09	3.98	2.71	-6.89
γ							
zethrene	0.05	5.4552	78.1	11.23	1.00	2.95	-13.70
dibenzoperylene II		5.23	80.0	10.19	0.64	2.82	-23.49
γ -bisanthrene		5.1683	84.3	9.73	0.92	2.62	-18.68
naphthocoronene		4.6554	81.8	7.83	3.98	2.32	-18.78
dibenzocoronene		5.22	82.5	10.25	4.80	3.01	-20.71
benzochrysenoperylene	0.15	5.133	82.1	10.56	3.90	2.67	-18.33
hexabenzocoronene		3.86	84.0	12.76	2.58	1.37	-16.04
γ'							
benzodiconene		3.8402	129.5	4.91	8.84	2.40	-31.55
tetrabenzoheptacene		3.86	20.0	1.16	12.88	2.05	-13.65 ^g
				12.76	2.58	1.37	-16.54 ^g
tetraazatetrabenzoheptacene		3.8517	25.3	0.50	11.56	5.68	-17.31 ^g
				12.46	1.45	2.97	-15.08 ^g
Triangular γ							
triphenylene		5.2694	88.1	1.79	1.71	6.21	-18.21 ^{g1}
			60.2	4.94	0.30	6.97	-9.10 ^{g2}
			55.0	0.54	7.25	4.28	-7.85 ^{g3}
			81.9	5.35	7.01	1.90	-7.18 ^{g4}
dibenzanthracene II		5.0623	91.8	3.32	5.17	5.12	-15.63 ^{g1}
			131.8	4.57	5.19	7.05	-10.02 ^{g2}
			85.6	4.41	0.77	6.02	-21.45 ^{g3}
			106.2	1.62	3.78	6.96	-19.02 ^{g4}
			137.3	7.22	2.31	4.75	-10.62 ^{g5}
Stack IIb (Pitched π -stack)							
benzopyrene II		4.556	106.8	9.60	1.50	4.10	-7.05
azabenzopyrene		4.608	108.7	9.45	1.69	3.92	-6.47
tetrabenzoanthracene		6.5062	64.8	0.81	1.36	8.01	-26.09
tetrabenzopentacene	(0.33) ^b	5.3214	80.0	3.21	10.46	6.78	-6.04
Quiones							
Stack III							
pyranthrone		3.79	7.2	5.50	7.71	2.65	-16.18 ^{p1}
			7.0	9.21	5.00	1.93	-18.39 ^{p2}

^a Field-effect hole mobility. ^b The BN-substituted form.

Table S3 Structure parameters of extended aromatic hydrocarbons with γ -structures before the φ -rotation

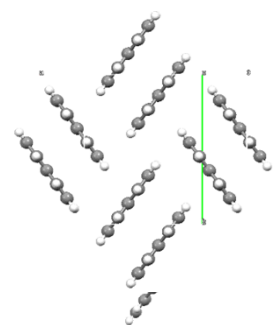
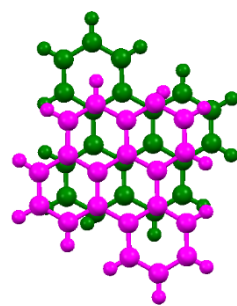
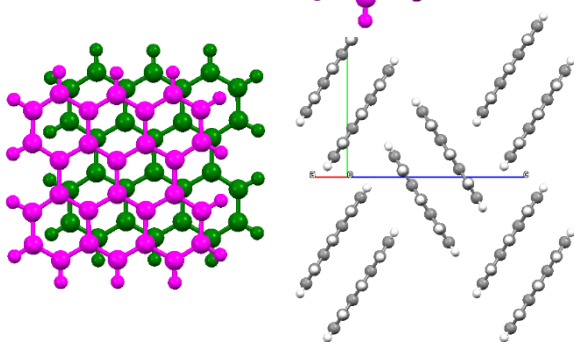
Compound	θ (°)	X_g (Å)	Y_g (Å)	Z_g (Å)	V_g (kJ mol ⁻¹)	X_s (Å)	Y_s (Å)	Z_s (Å)	V_s (kJ mol ⁻¹)	V_p (kJ mol ⁻¹)
zethrene	78.1	2.02	1.18	5.90	-27.85	0.28	4.21	3.45	-47.86	-13.70
dibenzoperylene II	80.0	4.58	0.27	7.34	-21.85	2.27	3.27	3.40	-63.62	-23.49
γ -bisanthrene	84.3	3.16	0.14	7.33	-20.67	3.79	0.86	3.40	-69.49	-18.68
	84.3	0.76	3.02	7.34	-21.37	1.27	3.67	3.41	-70.28	
naphthocoronene	81.8	5.68	0.14	8.38	-12.43	3.06	0.60	2.45	-84.43	-18.78
dibenzocoronene	82.5	4.01	0.96	7.21	-24.71	1.93	3.43	3.43	-81.30	-20.71
benzochrysenoperylene	82.1	3.29	1.80	7.28	-25.63	1.49	3.58	3.37	-88.85	-18.33
hexabenzocoronene	84.0	4.27	0.79	8.52	-22.57	3.80	0.18	3.42	-123.47	-16.04

(a) dibenzoperylene I (b) violanthrene (c) benzoperylene (d) terrylene



(e) bisanthrene

(f) benzopyrene I



(g) pyrene

(h) perylene

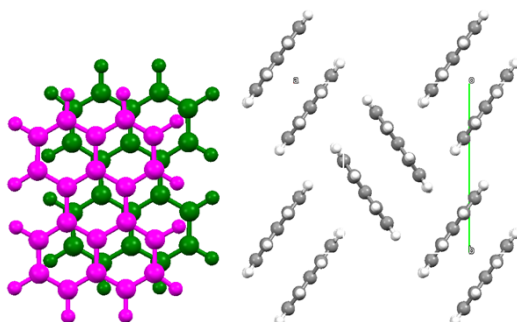
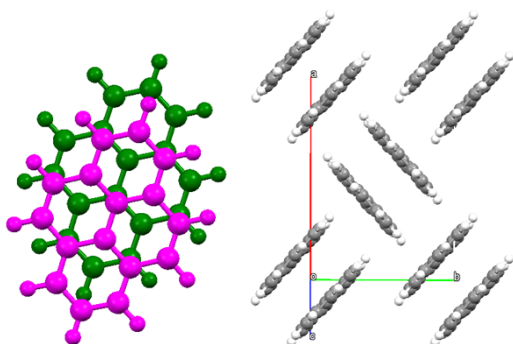
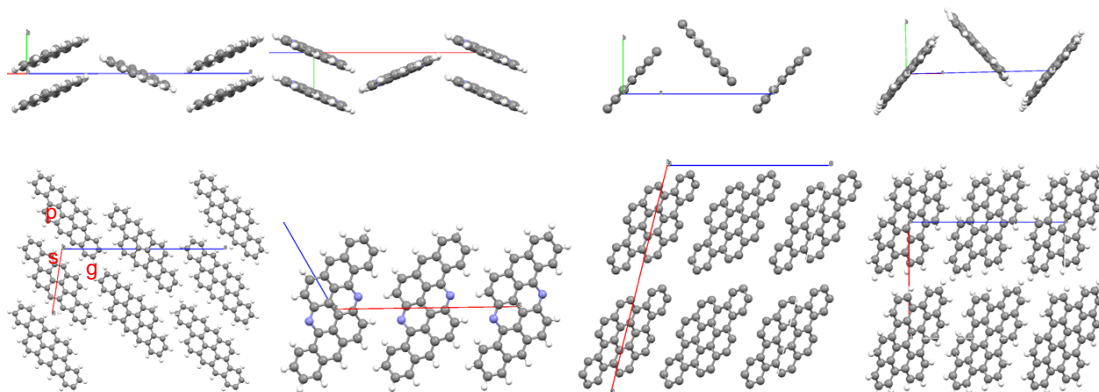


Fig. S2 Dimer and packing patterns of SHB structures in (a) dibenzoperylene I, (b) violanthrene, (c) benzoperylene, (d) terrylene, (e) bisanthrene, (f) benzopyrene I, (g) pyrene, and (h) perylene. In the dimer patterns, the layer (Y) direction is horizontal.

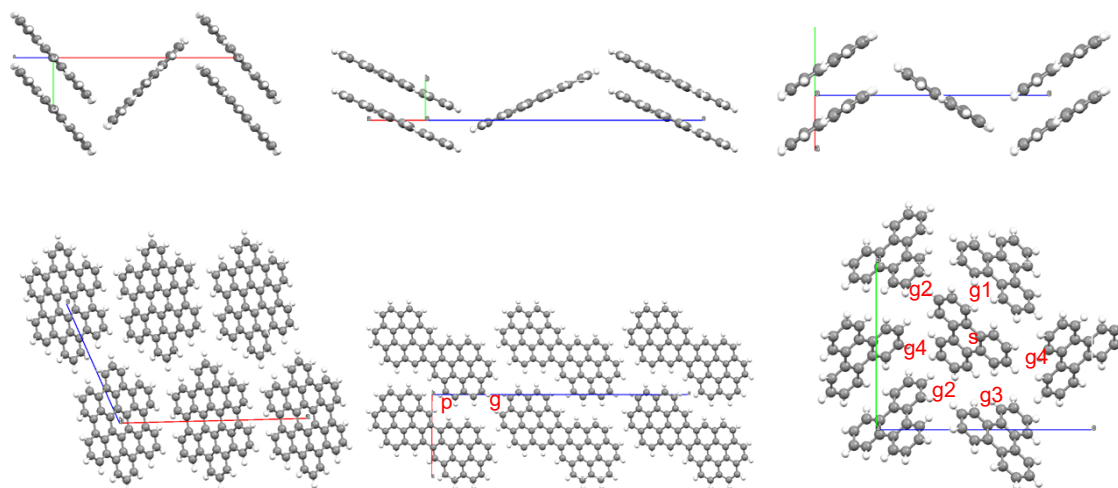
(a) tetracenotetracene (b) flavanthrene (c) dibenzocoronene (d) benzochrysenoperylene



(e) hexabenzocoronene

(f) benzodibenzocoronene

(g) triphenylene



(h) dibenzanthracene II

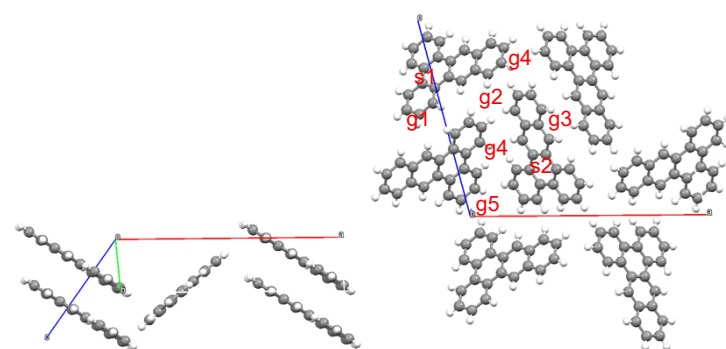


Fig. S3 Crystal structures of θ -structure (a) tetracenotetracene, and (b) flavanthrene, viewed from the molecular long axis and the stacking axis. Crystal structures of γ -structure (c) dibenzocoronene, (d) benzochrysenoperylene, (e) hexabenzocoronene, and (f) benzodibenzocoronene. Non-parallel contacts (g) are along the horizontal axis, whereas the vertical contacts are parallel (p). Crystal structures of triangular γ -structure (g) triphenylene, and (h) dibenzanthracene II.

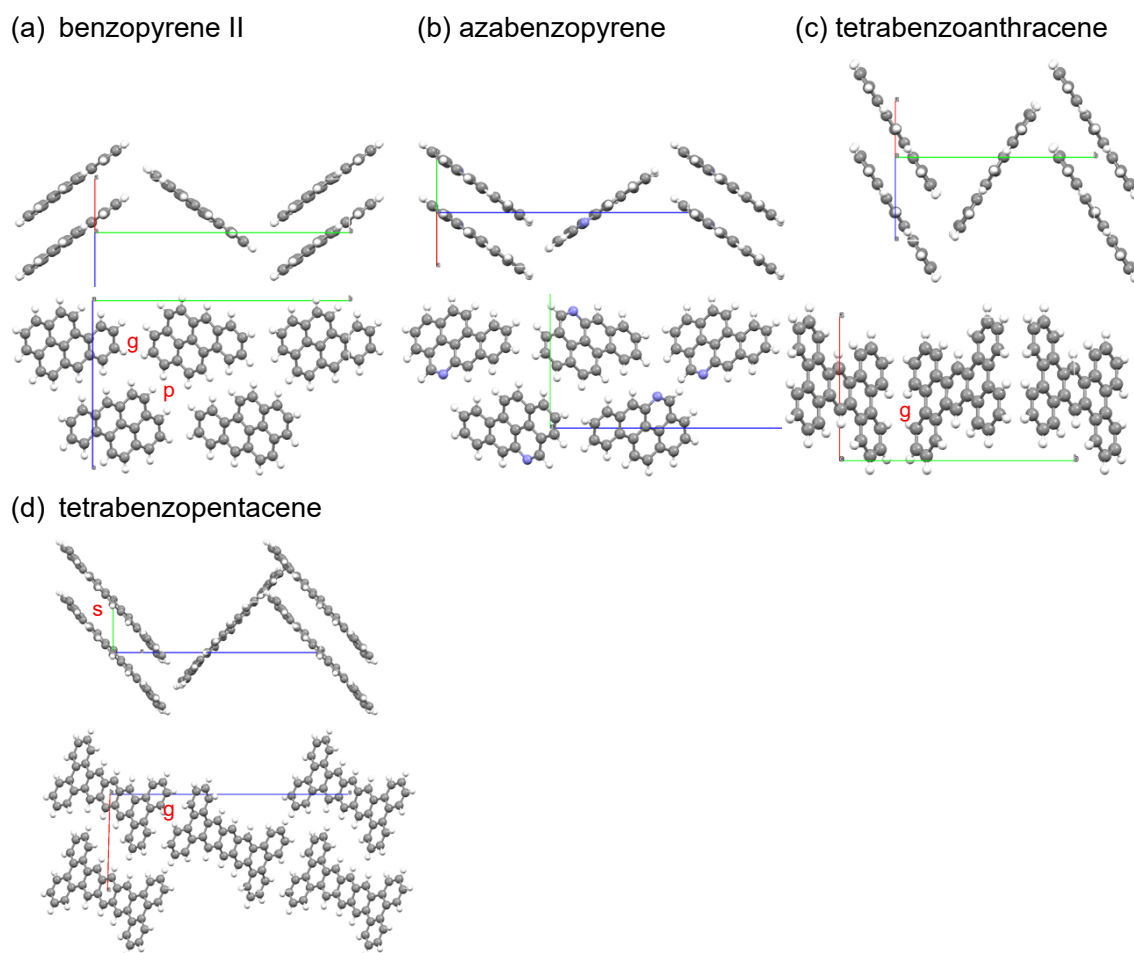
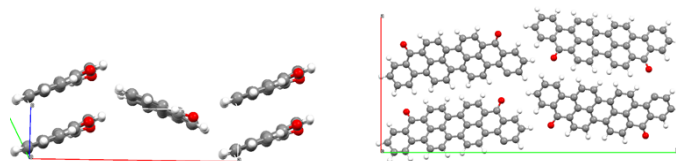


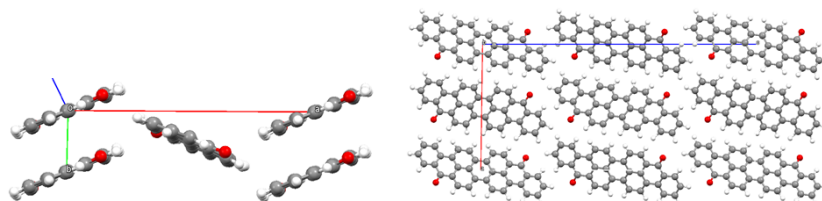
Fig. S4 Crystal structures of the pitched π -structures, viewed from the molecular short axis and the stacking axis. Non-parallel contacts are along the horizontal axis.

Azabenzopyrene has a similar molecular structure to benzopyrene II, but the crystal has a different space group. The pattern along the non-parallel axis (g) is almost the same, but the interaction along the parallel (p) axis is different.

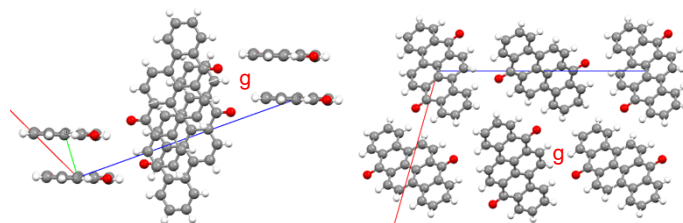
(a) isoviolanthrone



(b) violanthrone



(c) dibenzotetraphenenedione



(d) pyranthrone

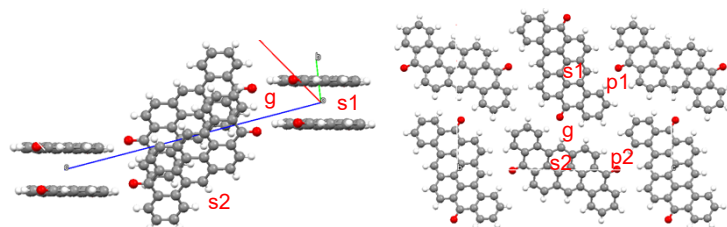


Fig. S5 Crystal structures of quinones viewed from the molecular long axis and the stacking axis.

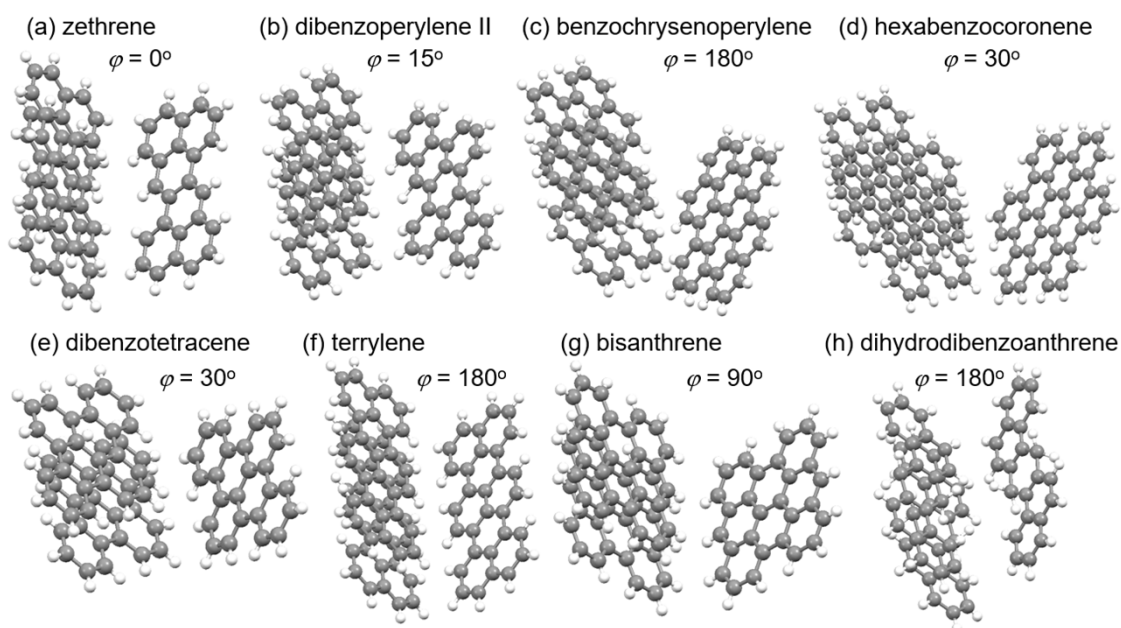


Fig. S6 Calculated molecular arrangements at the most stable φ (Fig. 5(b) and (c)).

In the γ structures, as shown in Fig. 5 and 8, the stacking and non-parallel molecules are rotated by φ around the central vertical (Z) axis of the original molecule. Since the molecule is not entirely circular, we have to modify X_0 and Y_0 to estimate the position of the stacking and non-parallel molecules according to eqns (1) – (4).

$$X_0^* = X_0 \cos^2 \varphi + Y_0 \sin^2 \varphi \quad (\text{S8})$$

$$Y_0^* = X_0 \sin^2 \varphi + Y_0 \cos^2 \varphi \quad (\text{S9})$$

Here X_0 and Y_0 are $L + 1.9 \text{ \AA}$ and $W + 1.9 \text{ \AA}$, respectively, and $\varphi = 0^\circ$ is defined by the direction with largest L . Fig. S6 and S8 depict the molecules generated by this way at $\theta = 90^\circ$. This calculation is extended not only to the γ -structure molecules but also to other molecules. For a rod-like molecule, $\varphi = 0^\circ$ (and 180°) affords a HB-like molecular arrangement (at $\theta = 90^\circ$, examples are Fig. S6(f), (h), S8(a), and (d)), whereas $\varphi = 90^\circ$ gives a pitched π -stack structure (an example is Fig. S8(c)).

Table S4 Supplementary structure parameters of compounds containing five-membered rings

Compound	μ_{max} (cm ² V ⁻¹ s ⁻¹) ^a	θ (°)	X_g (Å)	Y_g (Å)	Z_g (Å)	V_g (kJ mol ⁻¹)	X_s (Å)	Y_s (Å)	Z_s (Å)	V_s (kJ mol ⁻¹)	V_s' (kJ mol ⁻¹)
HB											
diindenoperylene 110 K	0.02	54.5	4.93	1.27	5.55	-38.33	3.59	5.89	3.08	-38.72	
	0.1 e ⁹⁸		1.60	1.10	5.28	-49.30	1.50	5.80	2.76	-47.07	
			3.09	4.69	2.52	-43.33					
			1.34	4.63	2.46	-49.53					
θ										V_p	
indeno[1,2-b]fluoranthene		126.4					7.96	5.32	2.60	-13.90	
diindenopyrene I		130.0					7.97	6.39	2.26	-14.47	
acenaphtho[1,2-b]fluoranthene		133.3	3.73	5.59	4.43	-17.87	0.57	1.48	3.48	-70.69 ^{s2}	
							9.08	4.31	0.67	-12.18 ^{p1}	-6.48 ^{p2}
θ -DOPT		127.5					0.92	12.27	2.50	-7.45	
decacyclene		130.1					12.72	0.83	1.79	10.86	
θ -dicycloheptarubicene	0.082	121.1					6.26	8.20	2.22	-14.15	
DBDAP	1.3 e	122.4					5.61	1.63	6.49	-10.69 ^{e2}	
γ			Before the ϕ rotation								
acenaphtho[1,2-b]naphthylene		72.7	1.18	0.71	5.86	-25.07	0.03	4.68	3.45	-36.35	-12.77 ^p
γ -DOPT	0.01	82.3	7.97	0.69	6.25	-16.42	1.31	3.66	3.40	-79.58	-16.69 ^p
rubicene	0.32	84.2	4.21	1.32	7.31	-21.11 ^e	1.71	3.45	3.42	-60.59 ^{s1}	-18.97 ^p
							2.08	3.26	3.39	-62.16 ^{s2}	
			3.22	9.43	4.38	-15.15 ^e	0.0	1.66	3.58	-109.0	-
dithienodibenzopyracylene		73.8	5.16	9.49	3.88	-9.63	3.82	2.35	3.37	-75.27	
diindenopyrene II		90.0	3.70	1.01	7.02	-22.12 ^{e1}	2.77	2.02	3.43	-71.98	-10.37 ^p
										-6.84 ^{e2}	
γ'											
diindenochrycene		89.3					9.88	5.07	2.48	-7.19 ^p	
benzodina[1,2-b]fluoranthene		92.8	8.55	0.62	6.77	-20.62 ^{e1}	1.00	3.59	3.54	-86.26	
		92.8	12.72	2.17	2.06	-11.36 ^{e2}					
		104.0	3.62	7.83	3.34	-17.15 ^{e3}					
		104.0	4.62	4.24	6.89	-14.82 ^{e3'}					
		135.2	8.14	6.58	8.78	-9.92 ^{e4}					
triangular											
cyclpentatriphenylene		79.8	6.47	0.80	3.71	-16.31 ^{e1}	4.00	0.36	3.36	-39.44 ^{s1}	-20.18 ^{p1}
		99.4	1.79	5.61	2.74	-20.14 ^{e2}	1.99	3.47	3.39	-39.80 ^{s2}	-18.04 ^{e2}
		124.2	3.47	5.83	5.30	-11.53 ^{e3}					
dibenzofluoranthene I		67.9	2.18	-0.24	5.79	-31.28 ^{e1}	0.19	4.90	3.31	-45.39 ^{s1}	-27.26 ^p
		88.4	2.34	1.93	6.96	-18.90 ^{e2}	0.36	4.89	3.32	-45.45 ^{s2}	
		49.2	9.92	2.28	0.98	-14.19 ^{e3}					
		49.2	6.30	4.04	6.97	-13.12 ^{e4}					
Stack IIb (Pitched π -stack)										V_p	
dibenzofluoranthene II							1.11	8.94	2.10	-14.60	
dicycloheptapentalene							1.48	6.92	2.12	-11.96	
dibenzorubicene		90.9	7.37	7.37	3.65	-8.00	1.42	8.83	2.02	-14.08	

^a Field-effect hole mobility unless indicated as "e".

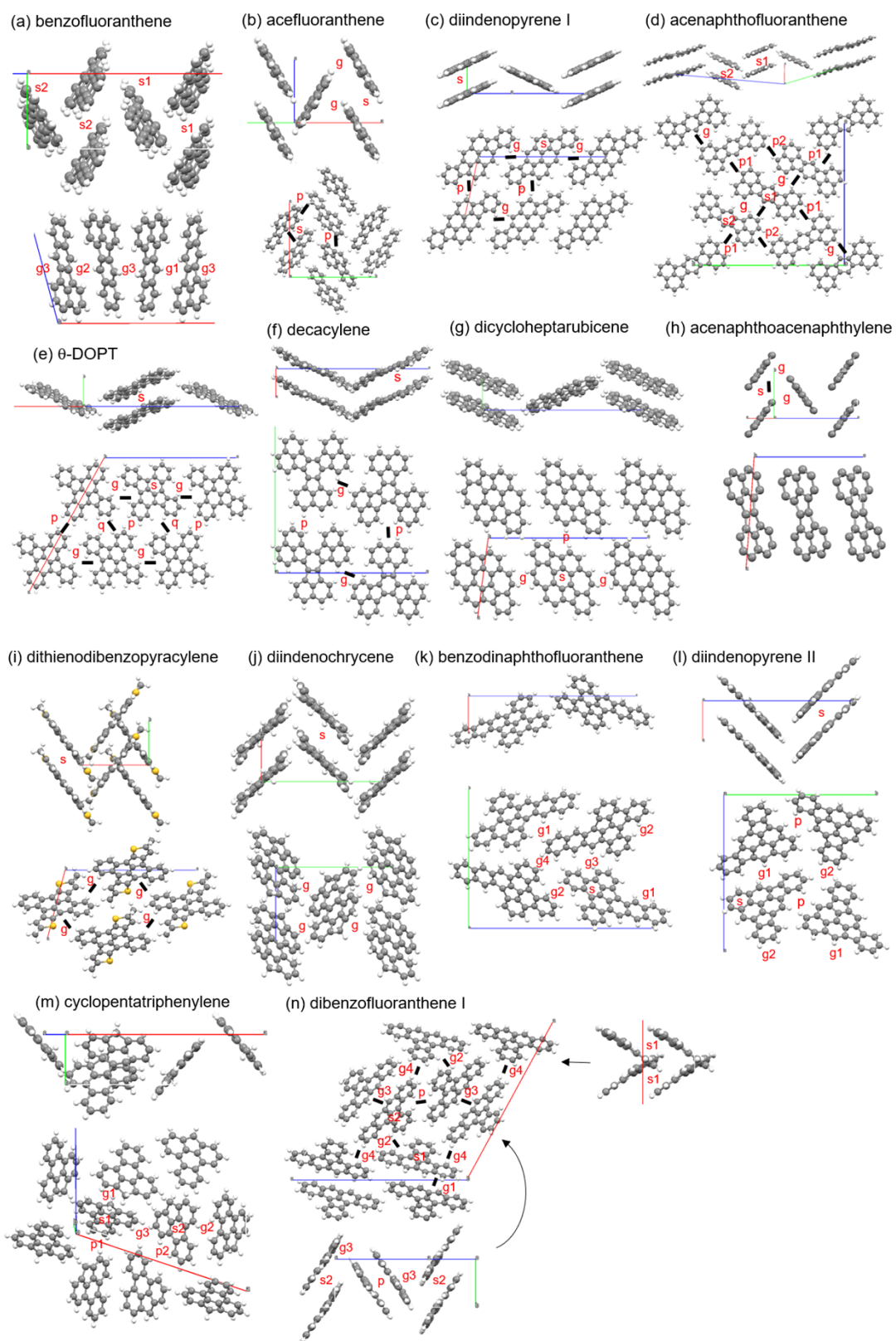


Fig. S7 Crystal structures of aromatic hydrocarbons containing five-membered rings. The marks such as g1-g4 and s1-s2 correspond to the interactions in Table 2 and S4.

In acefluoranthene, a stacking running along the c axis makes a HB-like arrangement (Fig. S7(b)), where the layer is perpendicular to the b axis. Although the two columns maintain the HB arrangement, the next two columns indicated by p are orthogonal.

In the θ -structure materials such as indenofluoranthene (Fig. 7(e)) and diindenopyrene I (Fig. S7(c)), X_g is large (Table 2). There is another transverse contact between parallel molecules, which is indicated as p in Fig. S7(c) and listed as V_p in Table S4. In acenaphthofluoranthene (Fig. S7(d)), three columns are θ -like, but the molecular long axes of the next three molecules are orthogonal.

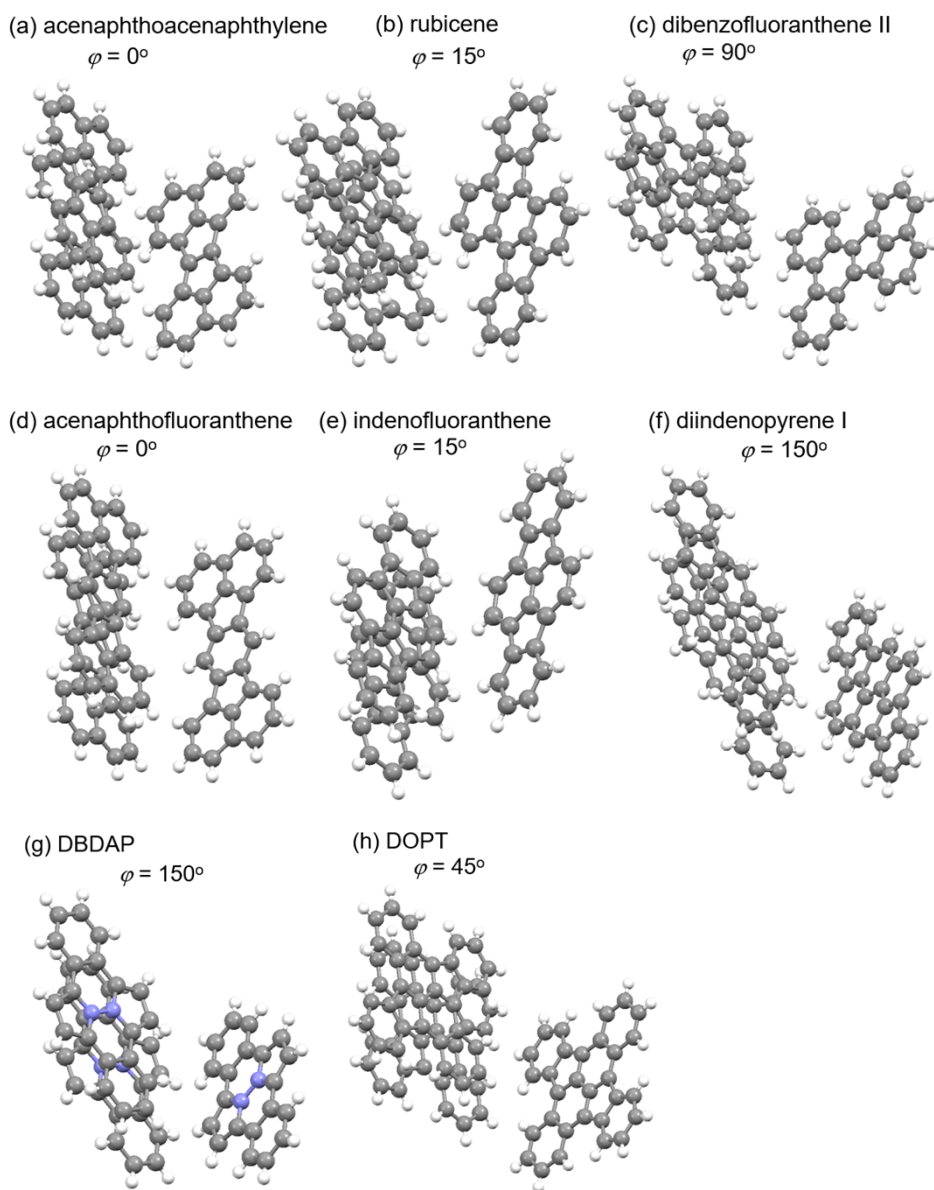


Fig. S8 Calculated molecular arrangements at the most stable φ (Fig. 8(b) and (c)).

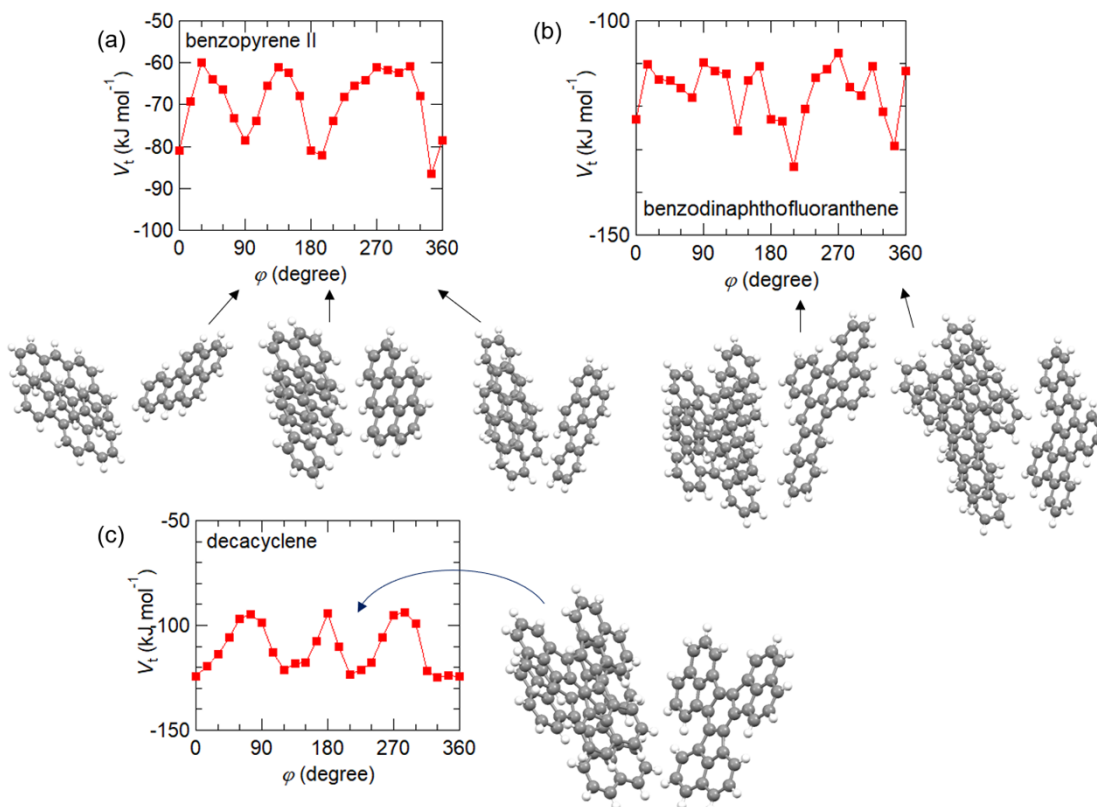


Fig. S9 ϕ dependence of V_t in (a) benzopyrene II, (b) benzodindaphthofluoranthene, and (c) decacyclene.

Due to the low symmetry of benzopyrene II, the ϕ dependence of V_t above 180° is not the repetition of the pattern below 180° (Fig. S9(a)). The 195° and 345° minima correspond to the long edge contact, but the actual crystal has a pitched π -stack structure, which is close to the 90° minimum. In a similar way, benzodindaphthofluoranthene affords several minima, among which the 345° minimum is close to the actual arrangement g1 (Fig. S7(k)). Decacyclene has 120° periodicity due to the molecular structure, and the minimum corresponds to the actual non-parallel contact g using the long edge (Fig. S7(f)).

Stability of SHB

In Table S5, energies of the actual SHB in dibenzoperylene I and anthanthrene are compared with those of the hypothetical γ (90°) and HB (60°) structures (Fig. S10). The order g2/g1 is opposite to Table 1. Energy of SHB is

$$V_t = 2(V_{g1} + V_{g2}) + V_{s1} + V_{s2} \quad (\text{S7})$$

for four molecules. $V_{t1} = 2V_{g2} + V_{s1}$ (Entry 1) is larger than $V_t = 2V_g + V_s$ (Entry 4) of the γ -structure because $X_s = 1.84$ (1.23) Å of SHB is smaller than $Y_s = 3.38$ (3.37) Å of the γ -structure. $V_{t2} = 2V_{g1} + V_{s2}$ (Entry 2) is comparable to the HB structure (Entry 5) because the geometry is not largely different. The SHB structure is a hybrid of the γ - and HB structures. The θ dependence of anthanthrene in Fig. S10(a) is flat in comparison with that of anthracenoanthracene in Fig. S10(b) and pentacene in Fig. 2(a); the latter two are HB compounds. If the twice of the 60° or 90° interaction (Entries 4 and 5) is not remarkably larger than the average (Entry 6), SHB (Entry 3) is preferable because the energy gain due to the dimer interaction (s1) is larger than the largely displaced stacking interaction of the γ -structure. Then in 2- and 2.5-leg molecules, the SHB structure is achieved instead of the HB structure.

Table S5 Structure parameters of SHB dibenzoperylene I, and anthanthrene

Compound	Entry	X_g (Å)	Y_g (Å)	Z_g (Å)	V_g (kJ mol ⁻¹)	X_s (Å)	Y_s (Å)	Z_s (Å)	V_s (kJ mol ⁻¹)	V_t (kJ mol ⁻¹)
SHB		g2/g1			s1/s2			t1/t2		
dibenzoperylene	1	2.83	2.96	5.99	-20.51	1.84	0.06	3.43	-72.80	-113.82
	2	0.70	0.30	6.02	-35.12	2.38	6.61	3.05	-33.01	-103.25
sum	3				-55.63				-107.81	-217.07
γ 90°	4	0.28	3.53	6.90	-14.77	0.0	3.38	3.38	-66.20	-95.74
HB 60°	5	0.33	0.02	6.24	-26.75	0.0	5.37	3.10	-45.79	-99.29
sum	6				-41.52				-111.99	-195.03
anthanthrene	1	1.37	1.62	6.15	-20.97	1.23	0.89	3.47	-61.45	-103.39
	2	0.15	1.97	6.02	-29.62	1.22	7.40	2.71	-19.19	-78.43
sum	3				-50.59				-80.64	-181.82
γ 90°	4	0.83	3.03	6.40	-15.67	0.0	3.37	3.37	-52.02	-83.36
HB 60°	5	0.21	0.09	5.90	-26.58	0.0	5.24	3.03	-32.15	-85.31
sum	6				-42.25				-84.17	-168.67

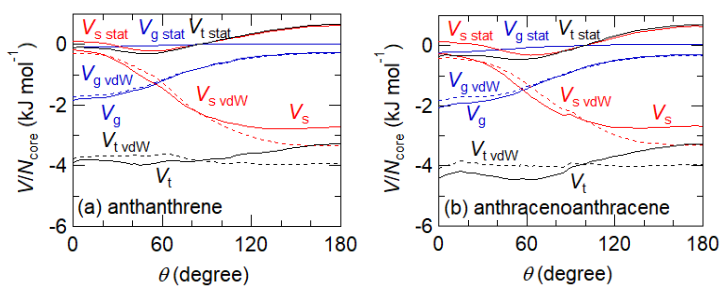


Fig. S10 θ dependence of (a) anthanthrene (SHB), and (b) anthracenoanthracene (HB).

References

- S1 A. Gavezzotti, *Acc. Chem. Res.*, 1994, **27**, 309.
- S2 M. Mirsky, *Acta Crystallogr. A*, 1976, **32**, 199.
- S3 D. E. Williams and T. L. Starr, *Computers Chem.*, 1977, **1**, 173.
- S4 S. R. Cox, L.-Y. Hsu and D. E. Williams, *Acta Crystallogr. A*, 1981, **37**, 293.
- S5 D. E. Williams and S. R. Cox, *Acta Crystallogr., Sect. B: Struct. Crystallogr. Cryst. Chem.*, 1984, **40**, 404.
- S6 W. L. Jorgensen and J. Tirado-Rives, *J. Am. Chem. Soc.*, 1988, **110**, 1657.
- S7 J. R. Holden, Z. Du and H. L. Ammon, *J. Comp. Chem.*, 1993, **14**, 422.
- S8 W. D. Cornell, P. Cieplak, C. I. Bayly, I. R. Gould, K. M. Merz, Jr., D. M. Ferguson, D. C. Spellmeyer, T. Fox, J. W. Caldwell and P. A. Kollman, *J. Am. Chem. Soc.*, 1995, **117**, 5179.
- S9 The software is available from <http://indigo1026.la.coocan.jp/lib/exp.html>. (accessed 12 December 2024).
- S10 <https://dasher.wustl.edu/tinker/distribution/params/> (accessed 12 December 2024).